

GHGT-11

Low-temperature CCS from an IGCC power plant and comparison with physical solvents

David Berstad<sup>a,\*</sup>, Rahul Anantharaman<sup>a</sup>, Petter Nekså<sup>a</sup>

<sup>a</sup>SINTEF Energy Research, 7465 Trondheim, Norway

**Abstract**

The application of low-temperature CO<sub>2</sub> capture has been investigated for an integrated gasification combined cycle (IGCC). The performance of low-temperature capture has been compared with Selexol capture for two different gasification technologies: pneumatic feed (G1) and slurry feed (G2). With low-temperature capture the resulting net electric efficiency for the IGCC with G1 and G2 gasifiers is 0.8 and 1.0 %-point higher than with Selexol. The improved efficiency indicates a clear advantage for low-temperature capture with respect to energy performance. Although further R&D is required, components and technology elements are existing and well known from other applications, indicating low technology barriers.

© 2013 The Authors. Published by Elsevier Ltd.  
Selection and/or peer-review under responsibility of GHGT

Keywords: CO<sub>2</sub> capture; IGCC; low-temperature; Selexol.

**1. Background and motivation**

The pre-combustion CO<sub>2</sub> capture route, through coal gasification or natural gas reforming followed by water-gas shift to synthesis gas with high CO<sub>2</sub> concentration and partial pressure, enables the use of other and more compact capture technologies than available for post-combustion. Baseline technologies for pre-combustion capture from IGCC are commonly assumed to be commercial physical solvent processes such as Selexol and Rectisol/methanol [1].

Despite physical solvents being proven and mature technology for CO<sub>2</sub> removal from synthesis gas, alternative technologies such as membranes, pressure-swing adsorption and low-temperature technologies have also been investigated in recent studies for pre-combustion. For low-temperature technologies different works have been presented on synthesis gas separation as well as oxy-derived flue gases with high CO<sub>2</sub> concentration.

In an effort to contribute to further reductions in energy penalties and cost of CO<sub>2</sub> capture from integrated gasification combined cycle (IGCC) plants, low-temperature synthesis gas separation has been further investigated as a novel alternative to state-of-the-art capture technologies.

\* Corresponding author. Tel.: +47-735-93934; fax: +47-735-93950.  
E-mail address: [david.berstad@sintef.no](mailto:david.berstad@sintef.no).

Recent conceptual studies [2–4] have pointed out advantageous features for low-temperature CO<sub>2</sub> capture by partial condensation and phase separation of synthesis gas. Important potential advantages are:

- No solvents required in the CO<sub>2</sub> capture unit
- High energy efficiency
- Compact capture unit
- Process equipment is mature and available

Initial results have shown that the equipment size can be reduced by 50–75% compared to physical absorption [2], and the energy penalty under certain conditions reduced by at least 30% [3]. In order to obtain a more exact and fair comparison it is however crucial to ensure comparable boundary conditions between the physical solvent and low-temperature processes, as well as implementing the capture process models in a defined IGCC power cycle. The main objective of this work is therefore to present a consistent comparison of the energy performance of the physical solvent Selexol and low-temperature synthesis gas separation for pre-combustion CO<sub>2</sub> capture from an IGCC power plant. A main focus has been on performing the energy benchmarking with equal and realistic boundary conditions, with respect to CO<sub>2</sub> capture rate (CCR) in particular.

Synthesis gas generated by two different gasification technologies, a Shell-type pneumatic-feed gasifier (G1) and a GE-type slurry-feed gasifier (G2), have been used as feed to the capture units. The overall energy performance of Selexol and low-temperature synthesis gas separation are evaluated and compared for both gasifier types.

## 2. Modelling and simulation

### 2.1. Vapour–liquid equilibrium data for the H<sub>2</sub>/CO<sub>2</sub> system

As discussed in previous works [3,4] the fraction of condensed CO<sub>2</sub> and thus obtainable CCR by phase separation of partially condensed synthesis gas is dependent on pressure and the temperature level at which the separation is carried out. Unfortunately, available thermodynamic data for H<sub>2</sub>/CO<sub>2</sub> systems and synthesis gas compositions is scarce and there are few published empirical studies against which equations of state (EOS) can be benchmarked. Experimental data for vapour–liquid equilibria of binary H<sub>2</sub>/CO<sub>2</sub> systems for relevant temperature and pressure range have been published by Spano et al. [5] and Tsang and Streett [6].

In this study, Peng–Robinson equation of state EOS has been used for all simulations of the low-temperature CO<sub>2</sub> capture unit. To relate the chosen EOS with experimental data, estimated CCR as function of pressure has been plotted in Fig. 1. With a constant separation temperature of -53.15°C (220 K), continuous lines represent estimated CCR for binary H<sub>2</sub>/CO<sub>2</sub> mixtures based on Peng–Robinson for three different CO<sub>2</sub> concentrations (38, 40 and 42%) while single data points are directly calculated from experimental vapour- and liquid-fraction data from [5] and [6] for 40% CO<sub>2</sub> concentration.

As can be observed, errors between the experimental and simulated data decrease with increasing separation pressure. However, synthesis gas compositions considered in this study are not binary H<sub>2</sub>/CO<sub>2</sub> systems but multi-component mixtures containing nitrogen, carbon monoxide and argon in addition to hydrogen and CO<sub>2</sub>. Hence, trends shown in Fig. 1 only serve as estimates for obtainable CCR. Based on this data a capture-unit CCR of 85% is targeted in this study and should be obtainable for the feed CO<sub>2</sub> concentrations available from the G1 and G2 gasifiers. Further discussion of experimental and simulated vapour–liquid equilibrium results can be found in [3].

It is assumed that the lowest temperature allowed for any process stream containing CO<sub>2</sub> is -56.16°C (217 K). Although freeze-out calculations must be handled with great care, it is assumed that this temperature is above the actual CO<sub>2</sub> solidification temperature at any point in the low-temperature processes. This is further discussed in section 3.

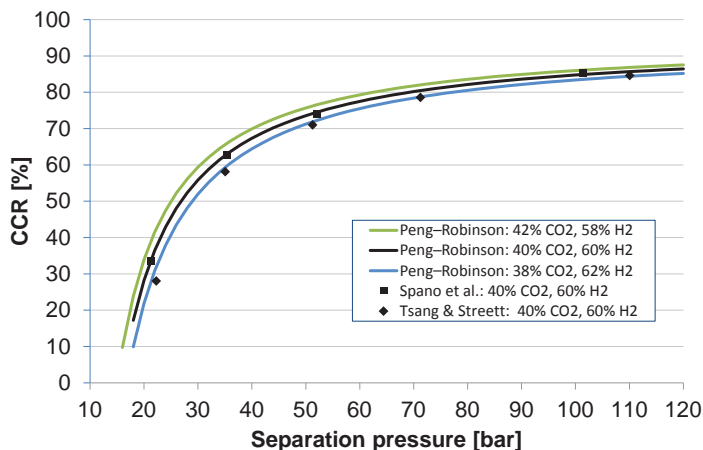


Fig. 1. Approximations of CCR for varying separation pressure and  $-53.15^{\circ}\text{C}$  (220 K) separation temperature. Calculations are based on binary  $\text{H}_2/\text{CO}_2$  mixtures.

## 2.2. Simulation tools

The IGCC power cycle and all other sub-processes including gasifier,  $\text{H}_2\text{S}$  removal and  $\text{CO}_2$  capture units are simulated as steady-state processes. The low-temperature  $\text{CO}_2$  capture units are simulated in Aspen HYSYS with Peng–Robinson EOS and standard models for all process units.

The gasification processes, power island and Selexol unit for  $\text{CO}_2$  capture and/or  $\text{H}_2\text{S}$  removal are all modelled in Aspen Plus. Peng–Robinson EOS is used for the gasifier island and gas streams, the Selexol process uses the PC-SAFT property method and STEAMNBS is used for the steam cycle. Main process parameters are declared in the following section.

## 3. Case study and process descriptions

Four case studies are considered in this work: G1 gasifier with Selexol capture, G1 with low-temperature capture, G2 with Selexol capture and G2 with low-temperature capture.

The principal process scheme for the IGCC with  $\text{CO}_2$  capture is shown in Fig. 2. A cryogenic air separation unit produces oxygen to the gasifier and inert nitrogen for use as diluent in the power island. For the pneumatic-feed G1 gasifier nitrogen is also used as transport gas for the lock hopper coal feed system while water is pumped for the slurry feed in gasifier G2. Sour water-gas shift is assumed for all simulated cases for both Selexol and low-temperature capture units.

The Shell-type G1 gasifier with Selexol unit for  $\text{CO}_2$  capture is considered the reference case in this work. In the case of  $\text{CO}_2$  capture by Selexol, the capture unit can selectively remove  $\text{H}_2\text{S}$  and  $\text{CO}_2$  in a two-stage process. This process is described in detail in [7] including all assumptions for process parameters. The GE-type G2 gasifier with Selexol unit for capture is discussed in detail in [8]. These reports [7,8] are used as the basis for simulations in this work.

For the IGCC cases with low-temperature capture, a dedicated Selexol desulphurisation unit is required prior to  $\text{CO}_2$  capture. Low-temperature co-removal of  $\text{CO}_2$  and  $\text{H}_2\text{S}$  is also an option but not further considered in this study. The sweetened synthesis gas streams entering the low-temperature capture unit are stated in Table 1 and a closer description of the low-temperature process follows.

The capture unit product streams consist of a  $\text{H}_2$ -rich gaseous product stream and captured  $\text{CO}_2$  stream. The  $\text{H}_2$ -rich stream is fed to the power island as gas turbine fuel while the stream of captured  $\text{CO}_2$  is transport-ready at 150 bar pressure after undergoing pressurisation either by multi-stage gas compression after Selexol-based capture or liquid pumping after low-temperature synthesis gas separation. Boundary conditions and assumptions specified in [7] are used for all four cases.

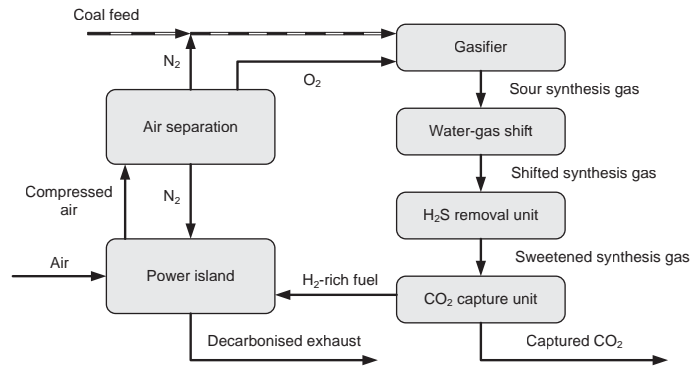


Fig. 2. IGCC process with pneumatic-feed gasification process, sour water-gas shift, desulphurisation and CO<sub>2</sub> capture.

Numerous process design options exist for CO<sub>2</sub> capture by partial condensation and phase separation of synthesis gas. The process scheme simulated for the cases of the present study is shown in Fig. 3 and feed stream data is listed in Table 1. After undergoing water-gas shift and H<sub>2</sub>S removal the synthesis gas is dried by regenerative molecular sieve adsorption before entering the capture unit in order to avoid potentially detrimental ice formation in the low-temperature part of the process.

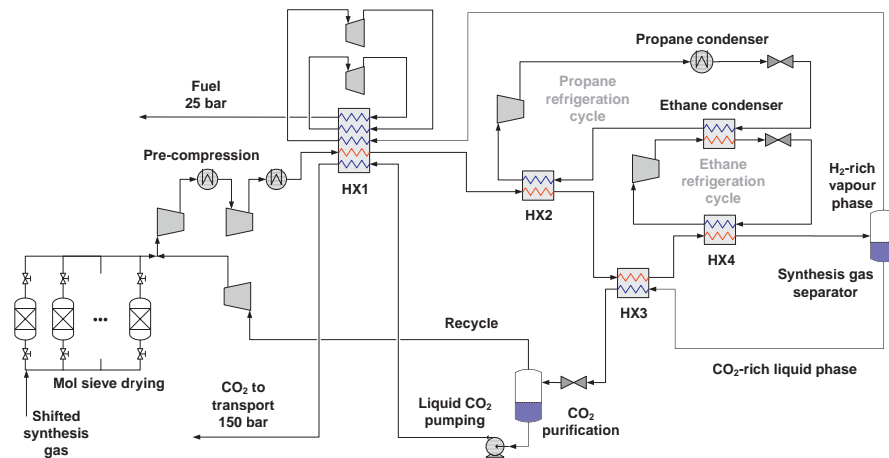


Fig. 3. Process flow diagram for the low-temperature CO<sub>2</sub> capture unit.

For the low-temperature capture cases a high separation pressure is required and pre-compression of the synthesis gas is carried out by one or two compression stages, depending on required separation pressure level. For gasifier G1 case a discharge pressure of 114.5 bar is assumed, corresponding to a discharge/suction pressure ratio of about 3.2. The maximum pressure ratio for a centrifugal compressor stage is, however, limited by the maximum impeller tip speed. Due to the relatively low molar mass of the hydrogen-rich synthesis gas at the compressor inlet, about 20.9 g/mol, the maximum pressure ratio calculates to 2.2–2.3 given a maximum specific enthalpy increase of 120 kJ/kg. With this constraint the G1 low-temperature case will require two compression stages as indicated in Fig. 3, while a single compression stage with a pressure ratio of 1.74 is sufficient for the gasifier G2 low-temperature capture case, operating with 93.5 bar discharge pressure.

Table 1. Compositions of sweetened and shifted synthesis gas fed to the low-temperature capture unit.

|    | Temperature<br>[°C] | Pressure<br>[bar] | Flowrate<br>[kmol/h] | Composition [mol-%] |                |                  |                 |       |                |       |
|----|---------------------|-------------------|----------------------|---------------------|----------------|------------------|-----------------|-------|----------------|-------|
|    |                     |                   |                      | CH <sub>4</sub>     | H <sub>2</sub> | H <sub>2</sub> O | CO <sub>2</sub> | CO    | N <sub>2</sub> | Ar    |
| G1 | 30                  | 36.1              | 20 362               | 0                   | 0.537          | 0.002            | 0.380           | 0.016 | 0.057          | 0.009 |
| G2 | 30                  | 54.3              | 19 593               | 0                   | 0.566          | 0.002            | 0.406           | 0.011 | 0.007          | 0.007 |

After pre-compression and cooling to 30°C by an ambient heat sink the synthesis gas enters the low-temperature heat exchanger network and is first cooled in a multi-stream process-to-process heat exchanger, HX1, against cold CO<sub>2</sub> and fuel product streams. As the partial condensation and separation of synthesis gas is carried out at high pressure, the H<sub>2</sub>-rich fuel stream is expanded down to 25 bar in two stages to generate cooling duty and recoverable shaft power.

The synthesis gas is subsequently cooled to about -39°C in HX2 and further to the final separation temperature in HX4 by a cascade propane and ethane refrigeration cycle. For the G1 case the separation temperature is specified to -56.15°C (217 K), while -55.15°C (218 K) is sufficient for obtaining a capture-unit CCR of 85% in the G2 case.

In order to purify the captured CO<sub>2</sub> stream and also minimise hydrogen losses in the low-temperature capture unit, the CO<sub>2</sub>-rich liquid product stream is further processed, first by re-heating through heat exchange against the synthesis gas stream in HX3. Furthermore, the CO<sub>2</sub> stream is then throttled to a lower pressure in a flash separator and stripped of dissolved hydrogen as well as nitrogen and argon. The flash gas stream, consisting of mainly CO<sub>2</sub> and H<sub>2</sub>, is recompressed and recycled back to the main feed stream, recovering a significant fraction of hydrogen otherwise lost with the CO<sub>2</sub> stream. Simulation results based on Peng–Robinson EOS give high CO<sub>2</sub> purities in the range of 99.7–99.9 mol-%. Final pressurisation of captured CO<sub>2</sub> to transport pressure is carried out by liquid pumping, thus avoiding far more energy-demanding gaseous compression.

The heating and cooling composite curves for the HX1–HX4 network are plotted Fig. 4. Due to differences in synthesis gas pressure as well as composition, there are slight differences in dew point temperature at which CO<sub>2</sub> starts to condense for the G1 and G2 cases. These differences in composition and pressure also result in different product-stream characteristics such as the available refrigeration duty per mass unit of H<sub>2</sub>-rich fuel generated across the dual expansion. Consequently profiles of the synthesis gas cooling curves as well as cold composite curves differ between the G1 and G2 cases.

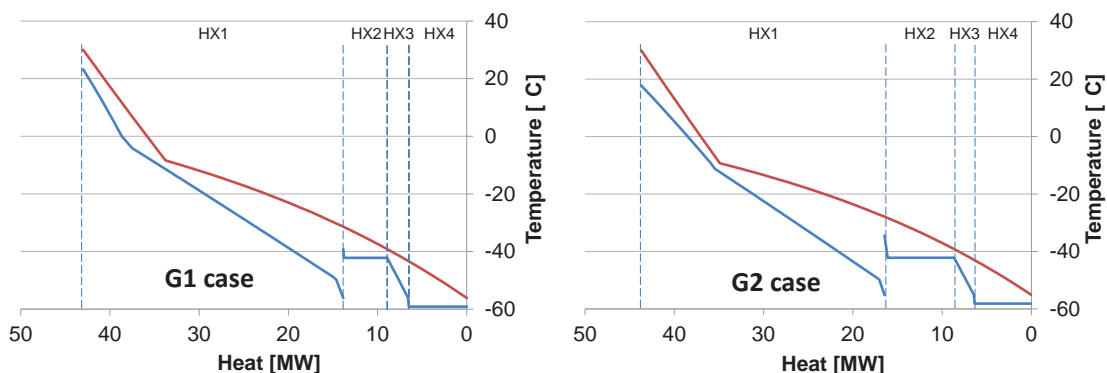


Fig. 4. Heat composite curves for synthesis gas coolers in the G1 and G2 low-temperature capture cases.

As can be observed, the major portion of the cooling duty for both cases is provided by process-to-process heat exchange in HX1. In each diagram in Fig. 4 the leftmost continuous cold curve for HX1 is the aggregate composite curve of cold process streams. Effective process integration and thus minimisation of auxiliary refrigeration power is a prerequisite for efficient low-temperature synthesis gas separation. Equally important is the recovery of shaft power from fuel expanders, in this work assumed to be recovered with 90% efficiency in conversion from mechanical to electrical power.

Main process parameters used in simulations of the low-temperature capture unit are listed in Table 2. These are considered to be conservative and realistic with respect to the process equipment needed in the unit. As discussed above in the section on vapour–liquid equilibrium, it is also assumed that the lowest allowed process-stream temperature of  $-56.16^{\circ}\text{C}$  (217 K) is within operational margins. With the process parameters assumed in the G1 and G2 cases, margins between stream temperature and estimated  $\text{CO}_2$  freeze-out temperature vary between 0.4 and  $2.7^{\circ}\text{C}$  in the concerned areas, that is, the feed and extraction points of the separators where the lowest temperatures are located. If larger margins between separation temperature and  $\text{CO}_2$  freeze-out temperature are required, this can be compensated for by raising the synthesis gas pressure and thus obtaining the targeted CCR with higher separation temperature.

Table 2. Main process assumptions for the low-temperature  $\text{CO}_2$  capture unit.

|  |     |     |  |                    |        |
|--|-----|-----|--|--------------------|--------|
| Mol sieve pressure drop                                      | bar | 0.5 | Fuel expanders, isentropic efficiency                              | %                  | 85     |
| Inter-cooler pressure drop                                   | bar | 0.5 | Fuel expanders, electric power recovery efficiency                 | %                  | 90     |
| Syngas pressure drop through low-temperature heat exchangers | bar | 2   | Minimum temperature approach in inter-coolers                      | $^{\circ}\text{C}$ | 15     |
| Syngas compressor 1st stage, isentropic efficiency           | %   | 85  | Minimum temperature approach, low-temperature heat exchangers      | $^{\circ}\text{C}$ | 3      |
| Syngas compressor 2nd stage, isentropic efficiency           | %   | 82  | Isothermal temperature difference in ethane condenser <sup>a</sup> | $^{\circ}\text{C}$ | 6.8    |
| Propane compressor, isentropic efficiency                    | %   | 85  | Cooling water temperature; temperature increase                    | $^{\circ}\text{C}$ | 15; 8  |
| Ethane compressor, isentropic efficiency                     | %   | 82  | Inter-cooler hot-side outlet temperature                           | $^{\circ}\text{C}$ | 30     |
| Recycle compressor, isentropic efficiency                    | %   | 80  | Minimum synthesis gas and $\text{CO}_2$ stream temperature         | $^{\circ}\text{C}$ | -56.15 |
| $\text{CO}_2$ pump, isentropic efficiency                    | %   | 80  | $\Delta T$ superheating for evaporators                            | $^{\circ}\text{C}$ | 3      |
| Cooling water pumps, efficiency                              | %   | 75  | $\Delta T$ sub-cooling for condensers                              | $^{\circ}\text{C}$ | 3      |

<sup>a</sup> between condensing ethane and boiling propane

#### 4. Main results and discussion

Main results for operational performance of the four cases are presented in Table 3. As can be observed, the Shell-type G1 gasifier configurations have higher efficiency than the corresponding configurations of the GE-type G2 gasifier. The G2 gasifier operates at a pressure of 58 bar compared to 40 bar in the G1 case, resulting in increased penalty for  $\text{O}_2$  compression work. Part of the increased energy requirement for high pressure G2 gasifier operation is recovered by expanding the gas turbine fuel to 25 bar and in  $\text{CO}_2$  compression. Another cause of energy penalty in the G2 gasifier case, compared to the G1 gasifier, is that G2 uses water quench leading to lower heat recovery by steam generation. The G2 gasifier uses slurry feed and thus does not require  $\text{N}_2$  compression as in the case of the pneumatic-feed G1 gasifier feeding system, as can be seen from Table 3. However, the slurry feed results in other inefficiencies in the overall IGCC process such as higher  $\text{O}_2$  consumption rate and thus higher energy penalty associated with cryogenic air separation.

The low-temperature capture unit, as explained, produces liquid  $\text{CO}_2$  as a product instead of capturing  $\text{CO}_2$  in gaseous phase, as is the case for Selexol. Thus, the compression work is included in the  $\text{CO}_2$  capture work given in Table 3 for the low-temperature cases. Moreover, the total  $\text{CO}_2$  capture work for the low-temperature unit is significantly lower than the sum of  $\text{CO}_2$  capture and compression work in the Selexol cases. This is the reason for the increase in efficiency for low-temperature cases relative to those with Selexol. Apart from these changes in values associated with  $\text{CO}_2$  capture and compression, most other values in the IGCC plant hardly change between the cases.

The overall CCR for the IGCC power plant calculates to 81.4% and 81.9% for the G1 case and 82.8% and 82.9% for G2. For the capture units a CCR of about 85% was specified based on the flowrate of captured CO<sub>2</sub> relative to the total flowrate of CO<sub>2</sub> fed to the capture unit. The reason lower overall CCR still becomes lower than 85% is the presence of CO in the process, not accounted for in the capture-unit notion of CCR. Hence, the overall CCR in Table 3 is based on captured *carbon* relative to that of the coal feed flowrate while capture-unit CCR is the ratio of captured CO<sub>2</sub> relative to the total CO<sub>2</sub> flowrate.

Table 3. Main results from simulated cases.

| Gasifier                               |          | G1             |                 | G2             |                 |
|--|----------|----------------|-----------------|----------------|-----------------|
| Capture process                        |          | Selexol        | Low-temperature | Selexol        | Low-temperature |
| Coal flowrate                          | tonnes/h | 136.6          | 136.7           | 140.9          | 141.3           |
| Coal lower heating value (LHV)         | MJ/kg    | 25.2           | 25.2            | 25.2           | 25.2            |
| Thermal Energy of fuel (LHV)           | MWth     | 955.1          | 955.8           | 985.4          | 988.1           |
| Thermal Energy for coal drying         | MWth     | 8.1            | 8.1             | 8.3            | 8.3             |
| Gas turbine output                     | MWe      | 283.1          | 284.3           | 282.7          | 282.9           |
| Steam turbine output                   | MWe      | 171.6          | 172.2           | 160.5          | 161.2           |
| Air expander                           | MWe      | 5.8            | 5.8             | 6.1            | 6.1             |
| GT fuel expander                       |          | —              | —               | 4.0            | —               |
| Gross electric power output            | MWe      | 460.5          | 462.3           | 453.2          | 450.2           |
| ASU power consumption                  | MWe      | 13.2           | 13.3            | 16.5           | 16.2            |
| O <sub>2</sub> compression             | MWe      | 11.6           | 11.6            | 22.4           | 22.4            |
| N <sub>2</sub> to gasifier compression | MWe      | 5.1            | 5.1             | —              | —               |
| N <sub>2</sub> to GT compression       | MWe      | 27.4           | 26.8            | 26.2           | 26.1            |
| CO <sub>2</sub> capture                | MWe      | 11.0           | 24.1            | 10.2           | 15.7            |
| Selexol – AGR                          | MWe      | included above | 0.3             | included above | 0.4             |
| CO <sub>2</sub> compression            | MWe      | 18.9           | —               | 19.2           | —               |
| Other                                  | MWe      | 10.8           | 11.1            | 13.0           | 13.0            |
| Total ancillary power                  | MWe      | 98.0           | 92.3            | 107.4          | 93.8            |
| Net electric power output              | MWe      | 362.5          | 370.0           | 345.8          | 356.4           |
| <b>Net electric efficiency</b>         | <b>%</b> | <b>37.6</b>    | <b>38.4</b>     | <b>34.8</b>    | <b>35.8</b>     |
| Overall CO <sub>2</sub> capture rate   | %        | 81.9           | 81.4            | 82.8           | 82.9            |
| Specific CO <sub>2</sub> emissions     | kg/MWh   | 175.1          | 177.5           | 174.2          | 174.0           |

## 5. Conclusions and needs for further research

Simulations of an IGCC power plant with two different gasifier technologies, pneumatic-feed (G1) and slurry-feed (G2), and two different CO<sub>2</sub> capture units, Selexol and low-temperature synthesis gas separation, have been performed. Overall CO<sub>2</sub> capture rates for the IGCC plant are 81.4–81.9% and 82.8–82.9% for the G1 and G2 gasifier cases, respectively. For these CCR values and with given process parameters, overall energy results for net electric efficiency show a significant advantage for the low-temperature CO<sub>2</sub> capture unit. Net electric efficiency for the IGCC plant with low-temperature CO<sub>2</sub>

capture is 38.4% and 35.8% with G1 and G2 gasifiers, respectively, and 0.8 and 1.0 %-points higher than for cases with Selexol CO<sub>2</sub> capture.

The low-temperature capture unit produces liquid CO<sub>2</sub> which is pressurised by liquid pumping and far less energy-demanding than gas compression, which is the case for Selexol. Although the refrigeration duties for synthesis gas cooling require considerable amounts of compression energy in the auxiliary refrigeration cycles, the net energy consumption still comes out lower for the low-temperature capture unit.

In addition to high energy efficiency the low-temperature concept has further potential features indicating advantageous cost characteristics, for instance process compactness due to high operating pressure and the avoidance of low, near-atmospheric suction pressure in the CO<sub>2</sub> compressor. Furthermore, reduced or possibly eliminated need for solvents and the maturity and availability of central process components also represent advantageous features about the low-temperature concept.

This study has been performed with available data for the different technologies and with realistic assumptions for component performance. There are, however, still areas which will require further research before a scaled-up implementation can be done. More accurate VLE and freezing point data for the relevant synthesis gas mixtures should be measured to define operational windows and constraints. Furthermore, unit operation testing to investigate deviations from equilibrium conditions should be performed as well as scale testing of the full low-temperature capture concept.

## Acknowledgements

This publication has been produced with support from the BIGCCS Centre, performed under the Norwegian research program Centres for Environment-friendly Energy Research (FME). The authors acknowledge the following partners for their contributions: Aker Solutions, ConocoPhillips, Det Norske Veritas, Gassco, Hydro, Shell, Statoil, TOTAL, GDF SUEZ and the Research Council of Norway (193816/S60).

## References

- [1] Intergovernmental Panel on Climate Change. *Carbon Dioxide Capture and Storage*. Cambridge: Cambridge University Press; 2005.
- [2] Brouwers J, van Kemenade H. Condensed Rotational Separation for CO<sub>2</sub> capture in coal gasification processes. *4th International Freiberg Conference on IGCC & xTL Technologies*. Dresden, Germany; 2010.
- [3] Berstad D, Nekså P, Anantharaman R. Low-temperature syngas separation for CO<sub>2</sub> capture from an IGCC power plant. *Proceedings of the 23rd IIR International Congress of Refrigeration (ICR)*. Paper 670; 2011.
- [4] Berstad D, Nekså P, Reigstad GA. Low-temperature syngas separation and CO<sub>2</sub> capture for enhanced efficiency of IGCC power plants. *Energy Procedia* 2011;4:1260–7.
- [5] Spano JO, Heck CK, Barrick PL. Liquid-vapor equilibria of the hydrogen–carbon dioxide system. *J Chem Eng Data*. 1968;13(2):169–71.
- [6] Tsang CY, Streett WB. Phase equilibria in the H<sub>2</sub>/CO<sub>2</sub> system at temperatures from 220 to 290 K and pressures to 172 MPa. *Chem Eng Sci* 1981;36:993–1000.
- [7] Anantharaman R et al. European best practice guidelines for assessment of CO<sub>2</sub> capture technologies. Public deliverable D1.4.3 in EU Project DECARBit; 2011.
- [8] Haslbeck JL et al. Cost and Performance Baseline for Fossil Energy Plants: Bituminous Coal and Natural Gas to Electricity Final Report. U.S. Department of Energy, Office of Fossil Energy, NETL, DOE/NETL-2010/1397; 2010.